DAPNIA/SEA-01-02
DESY TESLA-01-18

Collimation Depth Requirements for the TESLA Interaction Region

O. Napoly
CEA/Saclay, DAPNIA/SEA

12th February 2001

Abstract

The formalism for determining the rectangular beam collimation required by the clearance of the synchrotron radiation emitted in final focus quadrupoles is developed and applied to the case of the TESLA final focus system.

1 Collimation depths for uncoupled collimation and optics

We assume that collimation is provided by a pair of horizontal collimators with full gap ($g_x^{(i)}, i = 1, 2$) and a pair of vertical collimators ($g_y^{(i)}, i = 1, 2$) in such a way that both transverse planes and both phases are covered. The collimator gaps can be normalized with respect to the RMS beam sizes at the collimators

$$g_{x,y}^{(i)} = 2(N_{x,y}^{(i)} \cdot \sigma_{x,y}^{(i)})$$

The aim of the paper to determine the required values of the *collimation depths* $N_{x,y}^{(i)}$ such that the synchrotron radiation emitted by the collimated beam in the final doublet (or low-beta quadrupoles) is cleared by a given exit aperture in front of the doublet. This aperture can be the bore of the doublet itself, or the one of the opposite doublet, inboard or outboard of the IP, or some mask aperture.

Having considered an $x - y$ uncoupled geometry of the collimators, in contrast with circular collimators for instance, and assuming an uncoupled beam line optics in the beam delivery system (BDS), the tranverse phase-space distribution of the collimated beam at a given position s along the beam line, is $x - y$ decoupled :

$$\rho_\perp(X, Y; s) = \rho_H(X; s) \cdot \rho_V(Y; s)$$

with $X = (x, x')$ and $Y = (y, y')$. Also important is the collimated transverse phase-space domain which, for an uncoupled distribution, can be written as the cartesian product of the horizontal and vertical domains :

$$\mathcal{V}_\perp(s) = \mathcal{V}_H(s) \times \mathcal{V}_V(s)$$

To evaluate the impact of synchrotron radiation in the final doublet quadrupoles, we first need to characterize the electron phase-space domain $\mathcal{V}_\perp(s)$ for all positions s along the quadrupoles where photons are emitted. We will then propagate it, as if filled up by the photons, along a drift space through the relevant aperture. We will do this by transporting the electron collimated phase-space domain to the interaction point (IP), used as a reference point, and then backward to the doublet.

2 Phase-space domain of the collimated beam for linear optics

The derivation of the phase-space domain $\mathcal{V}_\perp(s)$ is a decoupled problem and we therefore work it out in one plane, say the horizontal one. The horizontal domain $\mathcal{V}_H(s)$ at any position s can simply be mapped from the acceptance of the two horizontal collimators :

$$\mathcal{V}_H(s) = \left\{ X \mid x^2(s^{(1)}) < (g_x^{(1)}/2)^2 \text{ and } x^2(s^{(2)}) < (g_x^{(2)}/2)^2 \right\}$$

with

$$x(s^{(i)}) = \left(M^{(i)}(s) \right)^{-1}_{11} (X)$$

where $M^{(i)}(s)$ is the 2×2 map from the collimator i to the position s. At the linear order, the map $M^{(i)}(s)$ is given by the transfer matrix $R^{(i)}(s)$ from the horizontal collimator i to the position s, and one can write :

$$x(s^{(i)}) = \left(R^{(i)}(s) \right)^{-1}_{11} (X) = R^{(i)}_{22}(s) x - R^{(i)}_{12}(s) x'$$

As a consequence, the phase-space domain $V_H(s)$ is the intersection of the stripes contained between the two parallel and symmetrical lines defined by

$$R^{(i)}_{22}(s) x - R^{(i)}_{12}(s) x' = \pm g_x^{(i)}/2$$

for each collimator i. In the case of two collimators, $\mathcal{V}_H(s)$ is in general a parallelogram. With n collimators, it is a $2n$-polygon with parallel opposite sides. These polygones are completely defined by the position of their corners which can be transported along the beam lines. In the doublet, the non-linear aberrations are expected to be small and we will use the linear optics to determine the domain $\mathcal{V}_H(s)$. Higher order or tracking studies must be done to validate this approximation.

As an intermediate step, we first derive the *linear* collimated phase-space domain $\mathcal{V}_H^*$ at the IP. Denoting by $R^{*(i)}$ the transfer matrix from the collimator i to the IP, the collimated phase-space domain at the IP is given by :

$$\mathcal{V}_H^*(s) = \left\{ X \mid \left(R^{*(i)}_{22} x - R^{*(i)}_{12} x' \right)^2 < (g_x^{(i)}/2)^2,\ i = 1,2 \right\}$$

It is the interior region of the parallelogram defined by the two pairs of parallel and symmetrical lines:

$$\begin{aligned} R^{*(1)}_{22} x - R^{*(1)}_{12} x' &= \pm g_x^{(1)}/2 \\ R^{*(2)}_{22} x - R^{*(2)}_{12} x' &= \pm g_x^{(2)}/2 \end{aligned}$$

Although it is independent of the choice of the matched beam conditions in the BDS, this system can be conveniently expressed in terms of the nominal Twiss parameters such that $\alpha_x^* = 0$ at the IP. Denoting by $\beta_x^{(i)}$the beta-function at the collimator i and by $\Delta\psi_x^{(i)}$ the phase advance from the collimator i to the IP, the system can be written as

$$\begin{aligned} x\sqrt{\frac{\beta_x^{(1)}}{\beta_x^*}} \cos\Delta\psi_x^{(1)} - x'\sqrt{\beta_x^{(1)}\beta_x^*} \sin\Delta\psi_x^{(1)} &= \pm N_x^{(1)} \sqrt{\beta_x^{(1)}\epsilon_x} \\ x\sqrt{\frac{\beta_x^{(2)}}{\beta_x^*}} \cos\Delta\psi_x^{(2)} - x'\sqrt{\beta_x^{(2)}\beta_x^*} \sin\Delta\psi_x^{(2)} &= \pm N_x^{(2)} \sqrt{\beta_x^{(2)}\epsilon_x} \end{aligned}$$

which can easily simplified into

$$\begin{aligned} x\cos\Delta\psi_x^{(1)} - x'\beta_x^* \sin\Delta\psi_x^{(1)} &= \pm N_x^{(1)} \sqrt{\beta_x^*\epsilon_x} \\ x\cos\Delta\psi_x^{(2)} - x'\beta_x^* \sin\Delta\psi_x^{(2)} &= \pm N_x^{(2)} \sqrt{\beta_x^*\epsilon_x} \end{aligned}$$

In general this system of equations defines a *finite domain*. Only if the phase advances from collimators 1 and 2 to the IP are exactly identical (single phase collimation) is the determinant of the above system zero

$$\Delta = \beta_x^* \sin\left(\Delta\psi_x^{(1)} - \Delta\psi_x^{(2)}\right)$$

and the domain an *infinite* stripe between the two narrowest parallel lines. Otherwise, this domain is the interior of a parallelogram. Since the parallelogram shape is invariant under charged (electrons) or neutral (photons) beam linear transport, its corners define the maximum extent of the charged beam and of the synchrotron radiation fan. The four corners are of course symmetric with respect to the origin and, denoting their coordinates by $(X_c^{*(+)}, X_c^{*(-)}, -X_c^{*(+)}, -X_c^{*(-)})$, the two independent ones are given by

$$X_c^{*(\pm)} = \begin{pmatrix} \frac{N_x^{(2)} \sin\Delta\psi_x^{(1)} \pm N_x^{(1)} \sin\Delta\psi_x^{(2)}}{\sin\left(\Delta\psi_x^{(1)} - \Delta\psi_x^{(2)}\right)} \sqrt{\beta_x^* \epsilon_x} \\ \frac{N_x^{(2)} \cos\Delta\psi_x^{(1)} \pm N_x^{(1)} \cos\Delta\psi_x^{(2)}}{\sin\left(\Delta\psi_x^{(1)} - \Delta\psi_x^{(2)}\right)} \sqrt{\gamma_x^* \epsilon_x} \end{pmatrix} \tag{1}$$

The volume of this phase-space domain is given by the following skew vector product,

$$V_H = \left|(X_c^{*(+)} + X_c^{*(-)}) \wedge (X_c^{*(+)} - X_c^{*(-)})\right| = \frac{4N_x^{(1)} N_x^{(2)} \epsilon_x}{\sin\left(\Delta\psi_x^{(1)} - \Delta\psi_x^{(2)}\right)} \tag{2}$$

It is of course invariant under electron and photon beam transport.

Of particular interest is the case when collimator 1 is at the doublet phase, i.e. $\pi/2$ from the IP, and collimator 2 at the IP phase. In this case, collimator 1 intercepts the most dangerous particles with a large offset in the doublet, while collimator 2 limits their angles in the doublet. The coordinates of the corners simplify to

$$X_c^{*(\pm)} = \begin{pmatrix} +N_x^{(2)} \sqrt{\beta_x^* \epsilon_x} \\ \pm N_x^{(1)} \sqrt{\gamma_x^* \epsilon_x} \end{pmatrix}$$

This implies that the parallelogram bounding $\mathcal{V}_H^*$ is a rectangle, as expected from the choice of the phase advances.

3 Phase-space domain of the synchrotron radiation

The corners of the phase-space domain $\mathcal{V}_H(s)$ at the location s in the doublet are then given by

$$X_c^{\pm}(s) = R^{-1}(s^*, s) \cdot X_c^{*(\pm)}$$

where s^* is the position of the IP and $R(s^*, s)$ is the transfer matrix from s to the IP. At this position, synchrotron radiation fills up the domain with photons which are emitted at the same position and, neglecting the small $1/\gamma$ angular opening of the cone of emission, with the same angle in such a way that the photon phase-space domain coincides with $\mathcal{V}_H(s)$.

The last step of the calculation consists in forward propagating the phase-space domain of the photons emitted at position s to the relevant aperture at the position L from the IP ($L > 0$ if downstream of the IP). This can be done by transporting the corners of $\mathcal{V}_H(s)$ through a simple drift space of length $(s^* + L - s)$. The corners of the photon phase-space domain $\mathcal{V}_H^\gamma(s, L)$ in this aperture are therefore given by

$$X_c^{\gamma\pm}(s, L) = D(s^* + L - s) \cdot R^{-1}(s^*, s) \cdot X_c^{*(\pm)} \tag{3}$$

where $D(l)$ is the transfer matrix of a drift with length l.

For a circular physical aperture of radius r, the transverse collimation depths are defined by the condition that, for all position s inside the upstream doublet, the longest diagonal in the $x-y$ collimated space fits the aperture circle, namely

$$\sup_{(\pm)} \left(x_c^{\gamma\pm}(s,L)\right)^2 + \sup_{(\pm)} \left(y_c^{\gamma\pm}(s,L)\right)^2 = r^2 \tag{4}$$

where $x_c^{\gamma\pm}$(respectively $y_c^{\gamma\pm}$) is the first coordinate of the 2D vector $X_c^{\gamma\pm}$ (respectively $Y_c^{\gamma\pm}$). Since $X_c^{\gamma\pm}$ and $Y_c^{\gamma\pm}$ are linearly related to the collimation depths $(N_x^{(1)}, N_x^{(2)})$ and $(N_y^{(1)}, N_y^{(2)})$ via Eqs.(1) and (3), the above equation (4) translates into a quadratic one for $(N_x^{(1)}, N_x^{(2)})$ and $(N_y^{(1)}, N_y^{(2)})$. Synchrotron radiation clearance is achieved when the collimation depths belong to the four dimensional domain defined as the intersection of the interior of all the 4D ellipsoids associated to all emission position s by the above equation 4.

The best values of $(N_x^{(1)}, N_x^{(2)})$ and $(N_y^{(1)}, N_y^{(2)})$ are of course given by the 3D surface which bounds this domain. But one still needs a criterion to define the *optimal* set of collimation depths. A natural criterion is to maximize the volume of the collimated phase-space $V_H \cdot V_V$, as given by Eq.(2). This leads to maximazing the product $N_x^{(1)} N_x^{(2)} N_y^{(1)} N_y^{(2)}$ which has the advantage to exclude the case where one collimator is closed and the associated depth is zero. But one could also devise alternative criteria motivated by physical constraints. For instance minimizing the wakefield effect of the collimators would, in a linear collider, lead to increase the vertical depths $(N_y^{(1)}, N_y^{(2)})$ at the expense of the horizontal ones $(N_x^{(1)}, N_x^{(2)})$.

4 Symmetric collimation in a circular aperture

The problem reduces to a 2D analysis in the case of *symmetric* collimation where both phases are collimated at the same depths, $N_{x,y}^{(1)} = N_{x,y}^{(2)} \equiv N_{x,y}$. From Eqs.(1) and (3), the coordinates $X_c^{\gamma\pm}$ and $Y_c^{\gamma\pm}$of the corners of the phase-space domain are then simply proportional to N_x and N_y, so that one can write

$$\begin{aligned} x_c^{\gamma\pm}(s,L) &= N_x \cdot \widehat{x}_c^{\gamma\pm}(s,L) \\ y_c^{\gamma\pm}(s,L) &= N_y \cdot \widehat{y}_c^{\gamma\pm}(s,L) \end{aligned}$$

The 4D ellipsoid equation (4) then simplifies to the following ellipse equation

$$\left(\frac{N_x}{N_x^{(0)}(s)}\right)^2 + \left(\frac{N_y}{N_y^{(0)}(s)}\right)^2 = 2 \tag{5}$$

where $N_x^{(0)}(s)$ and $N_y^{(0)}(s)$ are defined by

$$\begin{aligned} N_x^{(0)}(s) &= \frac{r}{\sqrt{2}\left|\sup_{(\pm)}\left(\widehat{x}_c^{\gamma\pm}(s,L)\right)\right|} \\ N_y^{(0)}(s) &= \frac{r}{\sqrt{2}\left|\sup_{(\pm)}\left(\widehat{y}_c^{\gamma\pm}(s,L)\right)\right|} \end{aligned}$$

For the particular solution $N_{x,y} = N_{x,y}^{(0)}(s)$ of Eq.(5), the synchrotron radiation fan emitted at position s fills the square inscribed in the circular aperture of radius r in the xy-plane. The values of $N_{x,y}^{(0)}(s)$ can easily be calculated and their minimum found numerically by splitting the final doublet into many slices. Selecting such a solution obviously maximimizes the product $N_x N_y$, and hence the collimated phase-space volume, as discussed in the preceding section.

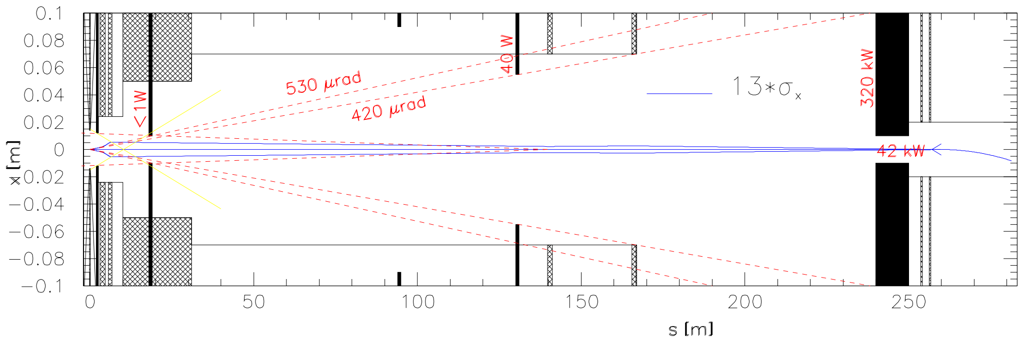

Figure 1: The layout of the TESLA interaction region and final focus system.

5 Application to the TESLA Interaction Region.

The TESLA interaction region is shown in Fig.(1). Starting from the IP ($s = 0$ m), the hatched areas show the last doublet (from $s = 3$ m to 6.7 m), the separators (from $s = 10$ m to 31 m), the last but one doublet (at $s = 140$ m and 165 m) and the first doublet (at $s = 254$ m and 256 m). The black areas show detector mask (at $s = 2$ m), the synchrotron radiation collimator (at $s = 18$ m) and the beamstrahlung dump (at $s = 240$ m). The synchrotron radiation collimator, with a circular aperture of 10 mm, shields the inner detector region from the photons emitted at any upstream magnets.

The ellipses in the two dimensional plane (N_x, N_y) are plotted in Fig.2 for the case of the last doublet with the TESLA 500 GeV parameters[1]. The values of the *square* collimation depths $(N_x^{(0)}, N_y^{(0)})$ are also shown as stars. Three different apertures are considered : the beam pipe at the vertex ($s = 0$ m, $r = 14$ mm), the exit of the opposite mask ($s = -2.6$ m, $r = 12$ mm) and, the exit of the opposite doublet ($s = -6.7$ m, $r = 24$ mm) . From this plot, the proper choice of the required *square* collimation depths is easy to derive by considering the smallest of the allowed values $N_x = 13.5$, $N_y = 82.3$. In the design of the TESLA collimation section, $13\sigma_x \times 80\sigma_y$ collimation depths have been assumed and the corresponding synchrotron radiation fan is shown in Fig.3. In the recent mask design, the inner mask has been brought closer to the IP with an exit at $s = \pm 2.4$ m which provides additional margin.

It is also interesting to investigate the impact of synchroton radiation emitted in the last but one doublet. Fig.4 shows that the optimal collimation depths derived for the final doublet is included in the allowed domain of the last but one doublet. This confirmed in Fig.5 by plotting the synchrotron radiation fan stemming from this doublet. Notice that the collimator at $s = 18$ m is also preventing the photons from the last but one doublet (and any upstream magnet) from hitting the inner detector. It is nevertheless useful because non-linear aberrations are large at this position, yielding particles with larger amplitudes than the linear collimation depths.

Aknowlegdments

I am indebted to R. Brinkmann, P. Emma and N. Walker for many clarifying discussions.

References

[1] Reinhard Brinkmann. High luminosity with TESLA 500. Technical Report TESLA 97-13, DESY, 1997.

TESLA 500 GeV (v08)

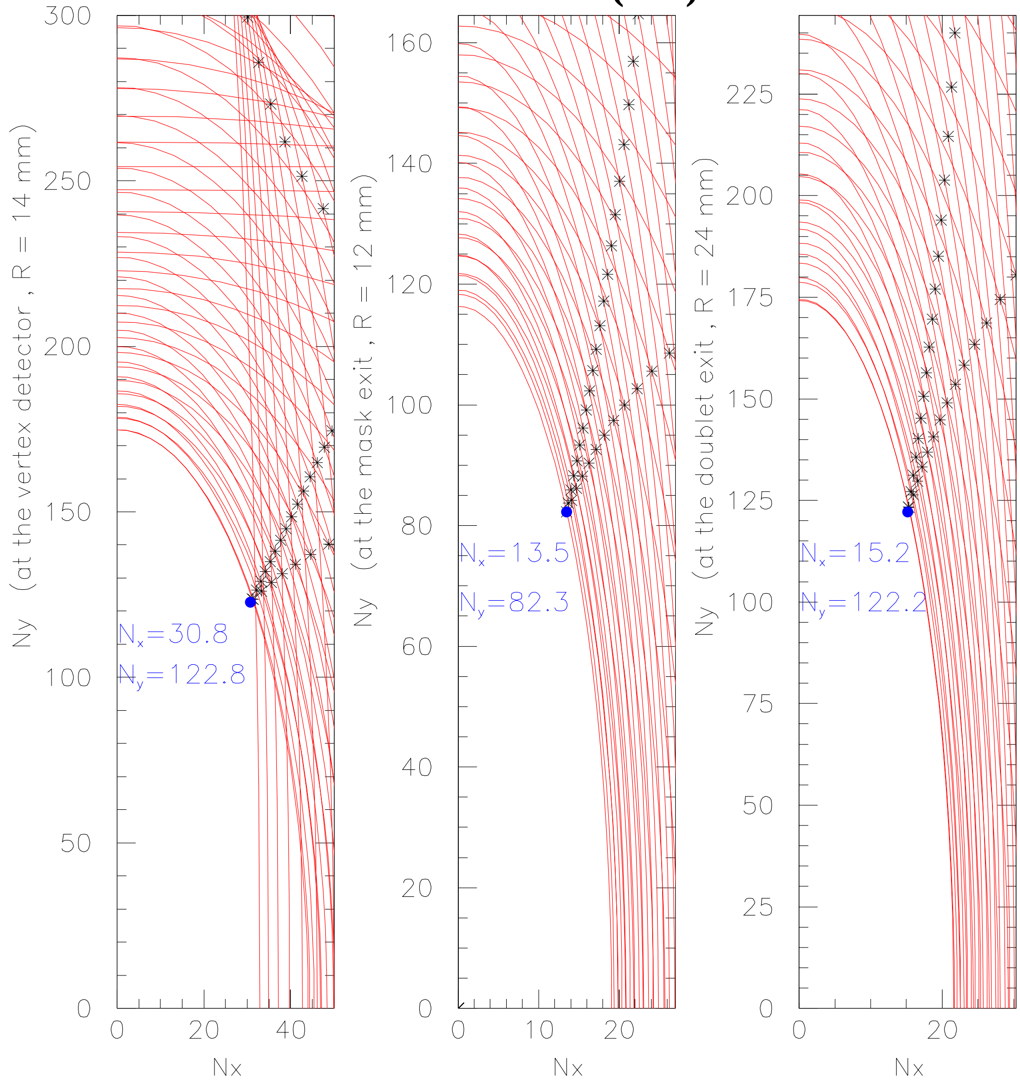

Figure 2: Allowed domain of collimation depths (N_x, N_y) for synchrotron radiation emitted in the last doublet. Ellipses are drawn as a function of the position s along the final doublet.

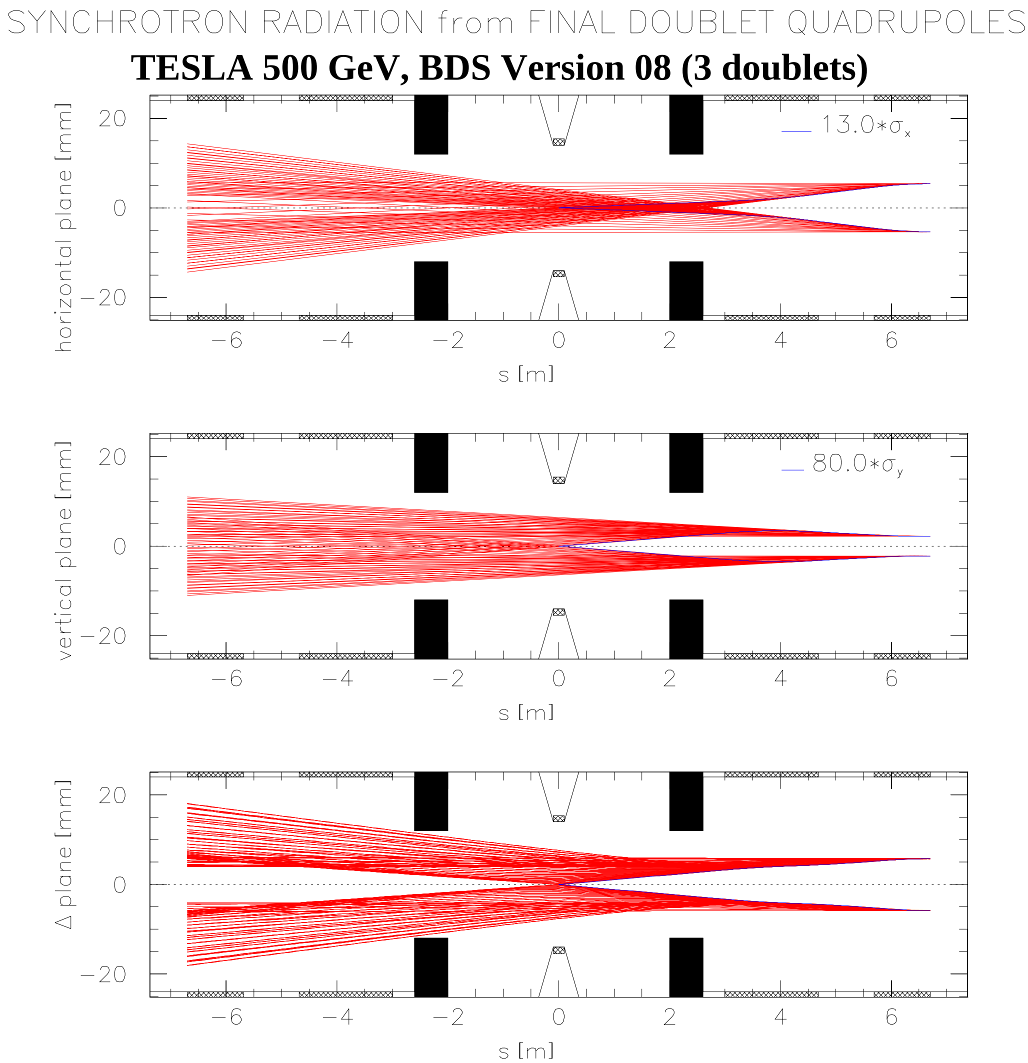

Figure 3: Synchrotron radiation fan from the last doublet through the TESLA IR. The bottom plot shows the diagonal extension of the corners of the photon phase space.

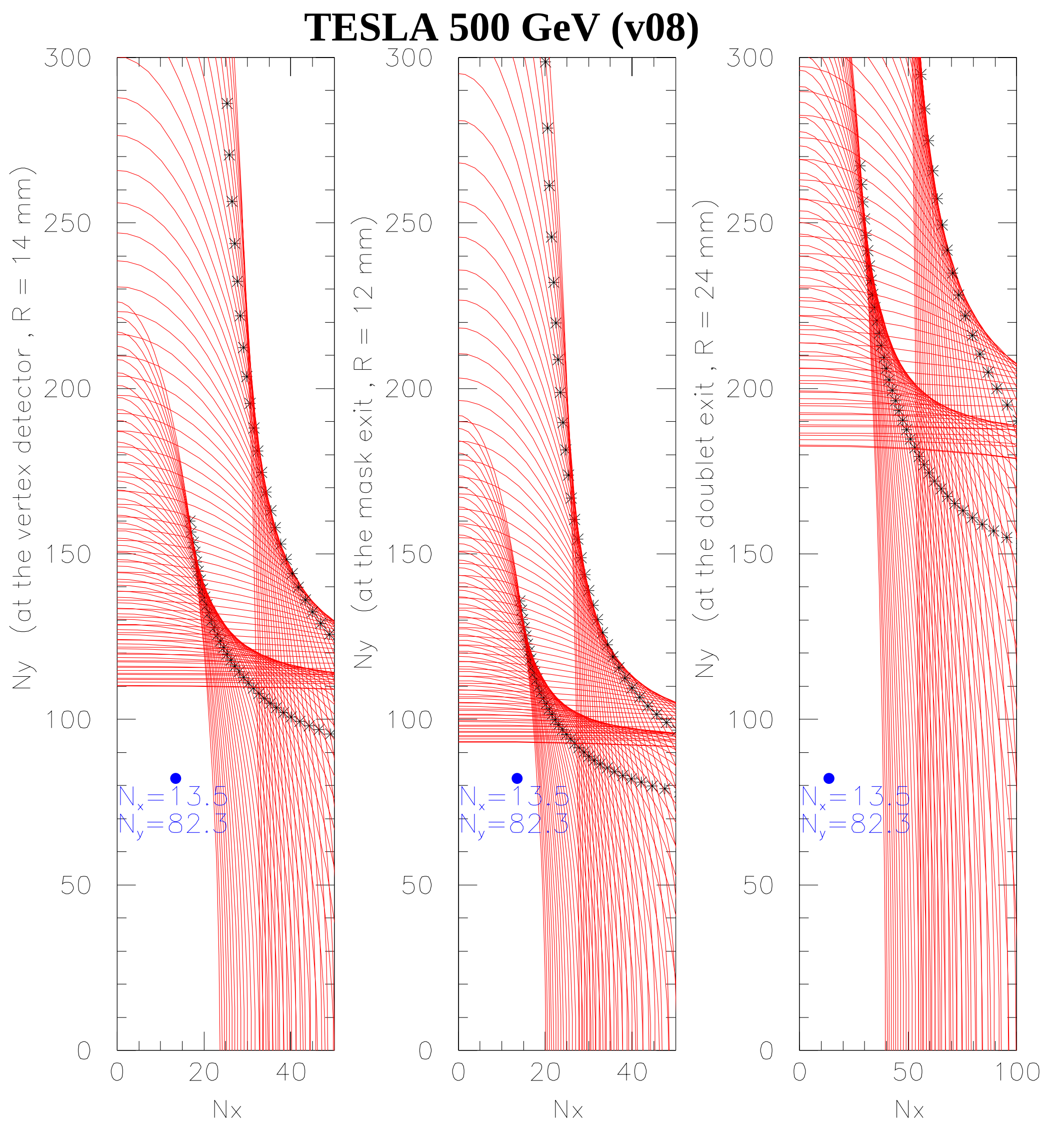

Figure 4: Allowed domain of collimation depths (N_x, N_y) for synchrotron radiation emitted in the last but one doublet. Ellipses are drawn as a function of the position s along the last but one doublet.

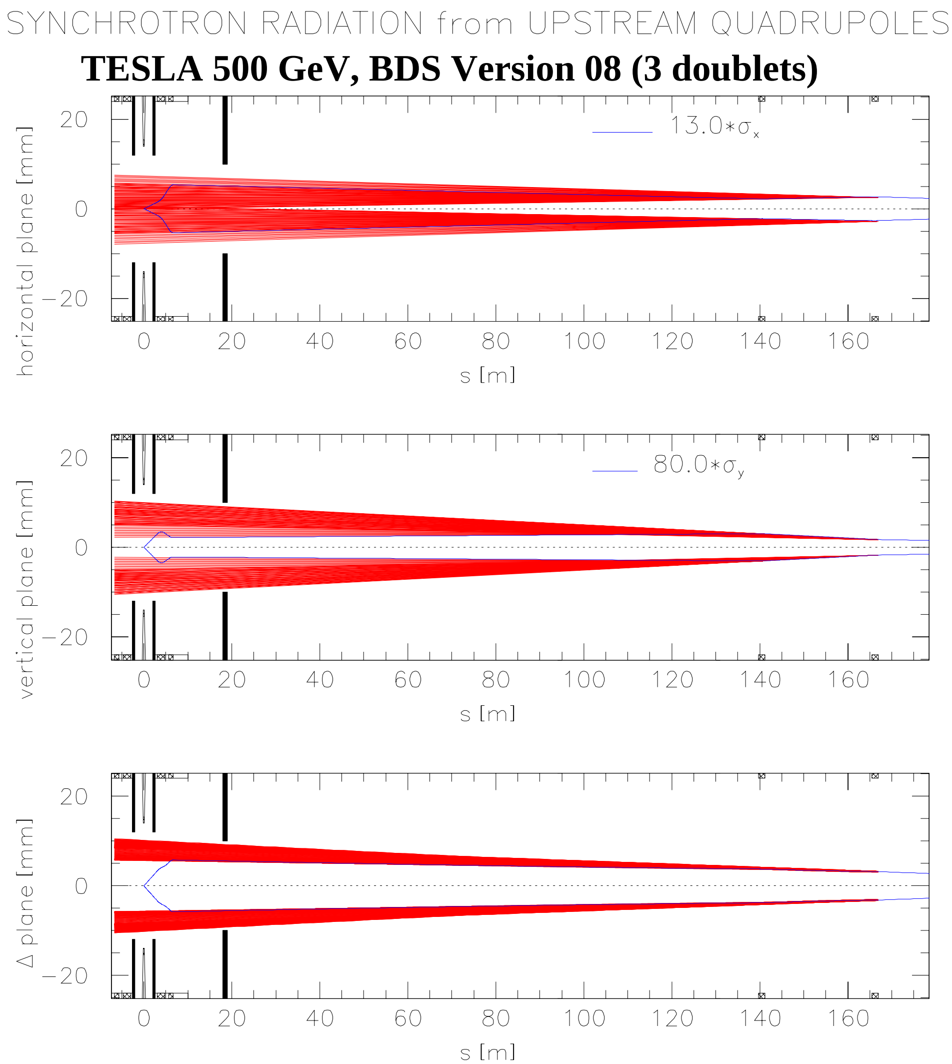

Figure 5: Synchrotron radiation fan from the last but one doublet through the TESLA IR. The bottom plot shows the diagonal extension of the corners of the photon phase space (for the sake of the plot, the last-but-one doublet a s = 140 m,165 m is shown with an aperture smaller than its real 70 mm bore radius).